

Analytical Methods

Accepted Manuscript



This is an *Accepted Manuscript*, which has been through the Royal Society of Chemistry peer review process and has been accepted for publication.

Accepted Manuscripts are published online shortly after acceptance, before technical editing, formatting and proof reading. Using this free service, authors can make their results available to the community, in citable form, before we publish the edited article. We will replace this *Accepted Manuscript* with the edited and formatted *Advance Article* as soon as it is available.

You can find more information about *Accepted Manuscripts* in the [Information for Authors](#).

Please note that technical editing may introduce minor changes to the text and/or graphics, which may alter content. The journal's standard [Terms & Conditions](#) and the [Ethical guidelines](#) still apply. In no event shall the Royal Society of Chemistry be held responsible for any errors or omissions in this *Accepted Manuscript* or any consequences arising from the use of any information it contains.

1
2
3
4
5
6
7
8
9
10
11
12
13
14
15
16
17
18
19
20
21
22
23
24
25
26
27
28
29
30
31
32
33
34
35
36
37
38
39
40
41
42
43
44
45
46
47
48
49
50
51
52
53
54
55
56
57
58
59
60

**A preanodized 6B-pencil graphite as an efficient electrochemical sensor for
mono-phenolic preservatives (phenol and *meta*-cresol) in insulin
formulations†**

Nandimalla Vishnu and Annamalai Senthil Kumar*

Environmental and Analytical Chemistry Division, School of Advanced Sciences,

Vellore Institute of Technology University, Vellore-632014, India

**Corresponding author's Fax: +91 416 2243092; Tel: +91 -416- 2202754;*

E-mail: askumarchem@yahoo.com

Abstract

Electrochemical oxidation of phenol on carbon electrodes has often been associated with problems such as serious adsorption, formation of electro-inactive tarry polymer and surface fouling. Thus, it is highly challenging to develop phenol electrochemical sensor without encountering such problems. Alternately, biosensors, those comprise of enzymes such as *tyrosinase* and *polyphenol oxidase*, were widely used for the aforesaid purpose. Here in, we introduce an ultra-low cost 6B grade pencil graphite, pre-anodized at 2 V vs. Ag/AgCl, designated as 6B-PGE*, where *=preanodized), as a novel electrochemical sensor for surface fouling-free and efficient differential voltammetric (DPV) detection of phenols (*meta*-cresol and phenol) in pH 7 phosphate buffer solution (PBS). A well-defined cyclic voltammetric peak at 0.65 ± 0.02 V vs. Ag/AgCl, which is stable under multiple electrochemical cycling, was noticed upon electrochemical-oxidation of *meta*-cresol and phenol at 6B-PGE*. The 6B-PGE* showed eight times higher DPV current signal and 60 mV lower oxidation potential than that of non-preanodized electrode (PGE) for the phenol detection. Under an optimal DPV condition, the 6B-PGE* showed a linear calibration plot with current linearity in a range 40-320 μM with current sensitivity and detection limit (signal-to-noise=3) values $1.43 \mu\text{A } \mu\text{M}^{-1} \text{ cm}^{-2}$ and 120 nM respectively. Six repeated detections of 80 μM *meta*-cresol without any interim surface cleaning process showed a relative standard deviation (RSD) value 0.21%. This electro-analytical approach was validated by testing total phenolic contents in three different insulin formulations containing with an electrode recovery value $\sim 100\%$.

Keywords: Preanodized pencil graphite; mono-phenol detection; insulin formulation; surface fouling-free.

1. Introduction

Human insulin is a polypeptide hormone secreted by pancreatic β cells, which is composed of 51 amino acids, 21-residue α -chain + 30-residue β -chain linked by two disulfide bonds.¹ It plays a key role in regulating the glucose metabolism.¹⁻³ Lack of control on insulin level in blood causes diabetes in which Type-I case patients depend on external insulin for their survival and while Type-II patients suffer from a "relative" insulin deficiency.⁴ As per the world health organization (WHO) about 347 million people worldwide have diabetes.⁵ Thus, dependency on external insulin flourished the insulin market by 7% of the annual rate and prospered with \$16.7 billion insulin sales.⁶ Generally, insulin is an unstable protein and is prone to degrade by microbes at room temperature.⁷ To prevent from the microbial degradation, about 3 mg mL⁻¹ phenolic preservative/s like *meta*-cresol, phenol and/or methyl paraben were often added to the pharmaceutical insulin.⁸⁻¹¹ Unfortunately, in some clinical cases, phenol and *meta*-cresol create adverse effects like allergy, urticaria, rash, angioedema, hypotension and dyspnea on patients health. If the *meta*-cresol is replaced with methyl paraben preservative, significant improvement in the clinical condition was noticed.¹⁰⁻¹² Furthermore, the phenolic preservatives in insulin were found to interacted with the polymer material used in the drug administration products and altered their bio-activity.¹¹ Thus, a simple and sensitive sensor for phenolic preservatives in insulin is highly needed for strict quality and quantity controls. Here in, we report a unique electroanalytical detection method using an ultra-low cost pencil as an efficient sensor for total phenol content in insulin formulations.

In the literature, separation coupled spectroscopic and electrochemical methods, in which high performance liquid chromatography and capillary electrophoresis as separation systems and UV-visible, fluorescence and amperometric i-t techniques as detectors, were often reported for

1
2
3 the phenolic compounds detection.¹³⁻¹⁹ Note that, the chromatography based detection techniques
4
5 are expensive and require large amount of high purity solvents and a well-trained technical
6
7 personnel.^{20,21} In addition, owing to its low absorption co-efficient, derivatization based
8
9 spectroscopic detection methods were widely used for sensitive detection of phenols.^{17,18} On the
10
11 other hand, electro-analytical detection technique offers simple, less-expensive and sensitive
12
13 analytical approach and it can be extendable to miniaturization as well.^{21,22} Unfortunately
14
15 electrochemical oxidative detection of phenols on solid electrodes like glassy carbon electrode
16
17 (GCE), platinum and gold follows tarry polymeric product and serious surface fouling problems
18
19 which then led to unstable current signals.^{23,24} For instance, Mathiyarasu et al reported about
20
21 80% decrement in the anodic current at ~ 1 V vs. Ag/AgCl and electro-inactive polymeric
22
23 products upon the electrochemical oxidation of 50 μ M phenol on a GCE surface in pH 7
24
25 phosphate buffer solution (PBS).²⁴ Note that the removal of the tarry polymers formed on the
26
27 electrode surface and electrode-renewal are tedious. Qin et al adopted repetitive CV cycling of
28
29 their working electrode at a potential window -0.4 to 0.8 V vs. SCE until background current
30
31 become constant as a cleaning step prior to the each measurements.²⁵ Recently, carbon nanotube
32
33 (CNT) modified GCEs were used for surface fouling-free electrochemical detection of mono-
34
35 phenols such as phenol and *para*-cresol.^{26,27} The graphitic impurity present in the CNT was
36
37 reported to be the key for the electrochemical detection. Nevertheless, high preparation cost and
38
39 tedious purification procedures are limitations of the CNTs for further analytical applications.²⁸
40
41 Meanwhile, phenol biosensors composed of specific enzymes like *tyrosinase*²⁹⁻³¹ and *polyphenol*
42
43 *oxidase*³²⁻³⁴ were reported for polymerization- and adsorption-free sensing of phenols in a neutral
44
45 pH solution. Besides, associated problems like instability in room temperature and complicated
46
47 purification methods and high cost often restrict the biosensors for cost-effective routine
48
49
50
51
52
53
54
55
56
57
58
59
60

1
2
3 analysis.³¹ As pointed out by Pumera and his co-workers and our group about the CNT's
4
5 graphitic impurity responsible for the phenol electrocatalytic oxidation reaction, here our interest
6
7 is to exploit an ultra-low cost pencil graphite as an alternative electrochemical sensor for the
8
9 mono-phenols.
10
11

12
13 Due to its low cost, good mechanical stability and electrical features, PGEs were often
14
15 utilized as electrochemical sensors in analytical chemistry.³⁵⁻⁴⁴ Table 1 provides existing
16
17 examples of various PGE modified systems used for the sensing of mono and diphenols
18
19 detections.^{35,37,38,42,43} Note that except with the 1.4 V activated PGE,³⁸ all other sensors
20
21 encountered serious surface adsorption complications.^{35,37,42,43} In fact, the 1.4 V activated PGE
22
23 also had surface renewability problem for the phenol detection.³⁸ Alternatively, fresh PGEs, as a
24
25 disposable sensor, were used for each measurements. Interestingly, a 2 V vs. Ag/AgCl pre-
26
27 anodized (in pH 7 PBS) 6B-pencil graphite, designated as 6B-PGE* where *=preanodized,
28
29 introducing in this work showed highly stable and selective detection of phenol unlike to the
30
31 previous electrodes with surface fouling and renewal problems in a neutral pH solution (Table
32
33 1). Using this new sensor, selective detection of phenol and *meta*-cresol in three different insulin
34
35 formulations were successfully detected with recovery values ~100%.
36
37
38
39
40
41
42
43

44 2. Experimental

45 2.1 Materials and Reagents

46
47 Insulin (>99% purity) and parafilm® M were obtained from Sigma-Aldrich, USA.
48
49 Phenol (≥98% purity), *meta*-cresol (≥98% purity), anhydrous sodium dihydrogen phosphate (≥98
50
51 % purity) and anhydrous disodium hydrogen phosphate (≥98 % purity) were procured from
52
53
54
55
56
57
58
59
60

Merck, Germany. Other chemicals were of analytical grade and used as received without any further purification. All the aqueous solutions were prepared using deionized and alkaline KMnO_4 double distilled water. Unless otherwise stated, pH 7 PBS of 0.1 M ionic strength was used as a supporting electrolyte. Different pencil of grades *viz.*, 2H, HB, B, 2B, 3B, 4B, 6B and 8B manufactured by Camlin, India were purchased from a local book store at VIT University campus. **Caution!** *Because phenols are corrosive, proper care must be taken during handling.*

2.2 Apparatus and preparation of working electrode

Voltammetric measurements were carried out using a CHI 440B electrochemical workstation, USA with 10 mL working volume. The three electrode system consists of a cylindrical pencil graphite (PGE) of dimension 3mm×40mm, where the cylindrical portion covered by a non-conductive parafilm leaving a disc portion (bottom) of geometrical surface area 0.0707 cm^2 , as a working electrode (Fig. S1†), Ag/AgCl with 3M KCl as a reference electrode and platinum wire as a counter electrode. Prior to the electrochemical measurements, the surface of 6B-PGE is mechanically cleaned by polishing with a bio-analytical system polishing kit (BASi, USA). 6B-PGE* is prepared by potentiostatic polarization of the PGE at an applied potential of 2 V *vs.* Ag/AgCl for 180 s in pH 7 PBS (Scheme 1, A and B). The optimized DPV parameters used for electrochemical detection of *meta*-cresol in this work are: initial potential=0.1 V; final potential=1.0 V; increment potential=0.004 V; amplitude=0.05 V; pulse width=0.2 s; pulse period=0.5 s. All the experiments were carried out in $25\pm 2^\circ\text{C}$ temperature.

Raman spectra was recorded using Peakseeker Pro Raman Spectrometer (Agiltron, USA) using a 532 nm laser probe. Fourier transform-infrared (FT-IR) spectral ($4000\text{-}400\text{ cm}^{-1}$) measurements were done by KBr pellet method using an IR Affinity-1 Fourier transform

1
2
3 Infrared spectrometer (Shimadzu, Japan). A D8 Advanced diffractometer (Bruker, Germany)
4
5 instrument with Cu K α source ($\lambda=1.5418 \text{ \AA}$) was used for X-ray diffraction (XRD) studies.
6
7
8
9

10 11 **2.3. Real Sample Analyses**

12
13 Three commercially available insulin samples *viz.*, soluble insulin injection I.P (Sample
14
15 #1; insulin-40 IU/mL+phenol-0.65 mg/mL+ *meta*-cresol-1.5mg/mL), biphasic isophane insulin
16
17 injection I.P (Sample #2; 40 IU/mL+phenol-0.65 mg/mL+ *meta*-cresol-1.5mg/mL) and isophane
18
19 insulin injection I.P (Sample #3; insulin-40 IU/mL+ *meta*-cresol-3.0 mg/mL) purchased from a
20
21 local pharmaceutical store in Vellore were used as real samples. For analysis, sample #1-#3 of
22
23 volumes 15, 10 and 15 μL respectively were directly added to 10 mL of blank pH 7 PBS and
24
25 subjected to quantitative measurements.
26
27
28
29
30
31

32 33 **3. Results and Discussion**

34 35 **3.1. Electrochemical and catalytic behaviors of the 6B-PGE***

36
37 Fig. 1A and 1B are continuous CV responses of 6B-PGE* with 160 μM *meta*-cresol (Fig.
38
39 1A, curve b) and phenol (Fig. 1B, curve b) in pH 7 PBS. An appreciable electrochemical
40
41 oxidation signal at $0.65\pm 0.02 \text{ V vs. Ag/AgCl}$ (irreversible type; A2 peak) with both, but a new
42
43 redox peak at $0.30\pm 0.02 \text{ V vs. Ag/AgCl}$ (reversible type; A1/C1 redox peak) selectively with
44
45 phenol, were noticed. After the electrochemical experiment, respective 6B-PGE*s were medium
46
47 transferred to a blank pH 7 PBS and were CV cycled again as in the curve c of Fig. 1A and 1B.
48
49 No redox response with *meta*-cresol-, whereas a specific surface confined redox peak at
50
51 $0.30\pm 0.02 \text{ V vs. Ag/AgCl}$ (A1/C1) with phenol-exposed 6B-PGE* were noticed. Qualitatively
52
53 similar CV responses were noticed if 6B-PGE* is subjected to DPV with phenol and *meta*-cresol
54
55
56
57
58
59
60

1
2
3 in pH 7 PBS (Fig. 1C, curves a and b). However, a quantitative comparison of CV and DPV
4 results was showed about 100 mV negative shift in the A2 peak potential with DPV, which may
5 be due to the pulse parameters such as increment potential, amplitude, pulse width and pulse
6 period used in this technique (Fig. 1C). It is obvious that electrochemical detection of *meta*-
7 cresol on the 6B-PGE* is freed from the serious adsorption and pre-peak problems, in this work.
8 Based on our previous report,²⁸ redox peak noticed at 0.25 ± 0.02 V vs. Ag/AgCl (A1/C1) with
9 phenol in this work can be assigned as a surface confined hydroquinone's redox species on the
10 6B-PGE*. This surface confined redox peak was found to be not interfering the phenol detection
11 peak noticed at 0.55 ± 0.03 V vs. Ag/AgCl (A2). Following conclusions can be drawn from the
12 above observations: (i) both *meta*-cresol and phenol oxidize at same magnitude (peak current and
13 potential are same) on 6B-PGE* in pH 7 PBS, (ii) a new surface confined peak is selectively
14 noticed with phenol oxidation (A1/C1), but not with the *meta*-cresol, (iii) the phenol oxidation
15 peak observed at 0.55 ± 0.03 V vs. Ag/AgCl (A2) is not interfered by the 0.25 ± 0.02 V vs.
16 Ag/AgCl peak (A1/C1) and (iv) *meta*-cresol is not active enough to form any surface confined
17 peak/s (A1/C1) on 6B-PGE*. Overall, the specific oxidation peak observed at 0.55 ± 0.01 V vs.
18 Ag/AgCl on 6B-PGE* is highly suitable for quantitative electrochemical detection of mono-
19 phenols in pH 7 PBS.
20
21
22
23
24
25
26
27
28
29
30
31
32
33
34
35
36
37
38
39
40
41
42

43 Initially, *meta*-cresol was taken as a model to study the phenol sensing by DPV
44 technique. Fig. 2A is a comparative DPV responses of 6B-PGE* and 6B-PGE for the detection
45 of 160 μ M *meta*-cresol in pH 7 PBS. As can be seen, the 6B-PGE* showed a well-defined
46 oxidation peak at 0.55 ± 0.01 V vs. Ag/AgCl (A2), which is 60 mV lower in potential and about
47 eight times higher in the peak current signal than the non-preanodized electrode, 6B-PGE. This
48 observation ascribes electrocatalytic feature of the 6B-PGE* for the *meta*-cresol oxidation in this
49
50
51
52
53
54
55
56
57
58
59
60

work (Fig 1A, curves a and b). In order to understand the surface feature, both 6B-PGE and 6B-PGE* were subjected to electrochemical (CV with $K_3[Fe(CN)_6]$) and physicochemical characterizations (XRD, Raman and FT-IR spectroscopies). Fig. 2B is a comparative CV responses of 6B-PGE* and 6B-PGE with 5 mM $K_3[Fe(CN)_6]$ at scan rate 10 mV s^{-1} in 0.1 M KCl solution. A well defined redox peak at an equilibrium potential, $E_{1/2} ((E_{pa}+E_{pc})/2) = 0.205 \pm 0.02 \text{ V vs. Ag/AgCl}$ with a peak-to-peak separation, $\Delta E_p = E_{pa} - E_{pc}$, where the E_{pa} and E_{pc} are anodic and cathodic peak potentials, $0.087 \pm 0.03 \text{ V vs. Ag/AgCl}$ were noticed with 6B-PGE*; while the values with 6B-PGE are $0.195 \pm 0.03 \text{ V vs. Ag/AgCl}$ and $0.106 \pm 0.03 \text{ V}$ respectively. The lower ΔE_p value observed with 6B-PGE* than the 6B-PGE denotes facile electron-transfer behavior of the preanodized system. Previously, it has been reported that preanodization of GCE and screen-printed carbon electrodes creates oxygen rich functional groups like, carbonyl ($>C=O$), phenolic (Ph-OH), alcoholic ($-C-OH$), carboxylic ($-COOH$) and ether ($-C-O-O-$) on its outer surface and further helps the promotion of electron oxidation/reduction of certain small molecules and biochemicals.⁴⁶⁻⁴⁹ It is expected that similar kind of oxygen functional groups might be formed on the surface of the 6B-PGE* and might be assisted the electrocatalytic oxidation of *meta*-cresol (Scheme 1C and 1D) in this work. In fact, observed two times higher back ground current signal with 6B-PGE* over 6B-PGE is due to the oxygen functional groups present on the 6B-PGE* surface (Fig. 2B).

3.2. Physicochemical characterization of the 6B-PGE*

To probe the surface characteristics, 6B-PGE* and 6B-PGE either in the form of powder or in native electrode were subjected to XRD, Raman and FT-IR spectroscopic characterizations. XRD of 6B-PGE* and 6B-PGE were showed broad 2θ peaks at 30 and 41° corresponding the

graphitic structures of the pencil (Fig. 3A). No significant variation in the XRD patterns was noticed before and after the preanodization procedure, which may indicate absence of any crystallinity change of graphitic structure against the preanodization. On the other hand, the XRD analysis is not sensitive enough to identify the generated functional group on the 6B-PGE* surface. Raman spectroscopic characterization is a powerful tool to probe the alteration in the graphitic structures. In general, graphitic materials display specific D and G bands at wavenumber ~ 1330 and 1570 cm^{-1} due to the disordered (sp^3 bonded sites) and ordered hexagonal carbon (sp^2 bonded sites) structures respectively and the intensity ratio of D and G bands, i.e., I_D/I_G can be taken as a measure for the graphitic disorder-ness.⁵⁰ Note that the oxygen rich functionalities such as quinone, phenol and alcoholic functional groups are responsible for the D band of the graphitic material. Fig. 3B is a comparative Raman spectroscopic responses of 6B-PGE and 6B-PGE* that showing D and G bands at 1351 ± 5 and $1568\pm 5\text{ cm}^{-1}$ as like conventional graphitic materials (CNT and graphite).^{50,51} Calculated peak intensity ratio, I_D/I_G values are 0.107 and 0.245 respectively for the 6B-PGE and 6B-PGE* samples. It is obvious that the 6B-PGE* has 2.3 times higher I_D/I_G ratio value than that of 6B-PGE. Conversion of some sp^2 graphitic units to sp^3 -carbon-oxygen functionalities is a likely reason for the higher I_D/I_G value. To support the result, powders of 6B-PGE and 6B-PGE* samples were further subjected to FT-IR characterization as in Fig. 3C. IR peaks corresponding to the hydroxyl ($-\text{OH}$, 3429 cm^{-1}), sp^2 carbons ($>\text{CH}=\text{CH}<$, 1633 and 1588 cm^{-1} and 1377 cm^{-1} (bending mode)) and $>\text{CH}_2$ (anti-symmetric and symmetric mode at 2920 and 2846 cm^{-1}) functional groups were noticed both with the 6B-PGE and 6B-PGE* samples.²⁸ Beside, IR peak intensities of the 6B-PGE* sample are significantly higher than the 6B-PGE. In particularly, about two fold enhancement in the ν_{OH} stretching signal at $3430\pm 5\text{ cm}^{-1}$ with 6B-PGE* over 6B-PGE was noticed (Fig. 3C, curves a and

1
2
3 b). These results confirm creation of oxygen rich functional groups on the 6B-PGE* upon the
4 pre-anodization process.
5
6
7

10 3.3. Effect of pencil grade

11
12 In general, pencils are made up of clay-graphite composite.⁵² It is expected that graphitic
13 part in the phenol is a key for the electrochemical activity in this work. To understand the
14 graphite contribution, different grade pencils viz., 2H, HB, B, 2B, 3B, 4B, 6B and 8B, where B
15 and H denotes hardness and blackness respectively (graphite/clay ratio increase with increase in
16 the B grade), were subjected to electrochemical detection of 160 μM *meta*-cresol as in Fig. 2C. It
17 is obvious that the grade of pencil has some influence on the phenol oxidation reaction. A linear
18 increase in trend between DPV peak current and pencil blackness, up to 6B grade, after that
19 decrease in the trend was noticed. With 8B-PGE*, problems like serious adsorption of the phenol
20 and surface fouling and hence remarkable decrement in the current signal, were obtained.
21
22 Meanwhile, the respective non-preanodized pencil graphite electrodes (PGEs of 2H-8B grades)
23 showed poor DPV signals for the phenol detection (Fig. 2C, curve b). Since the 6B-PGE* has
24 showed maximum peak current response, it is chosen as an optimal electrode for further
25 analytical studies in this work.
26
27
28
29
30
31
32
33
34
35
36
37
38
39
40
41
42
43
44
45

46 3.4. Analytical measurements

47
48 Interrelated DPV parameters were systematically optimized for *meta*-cresol detection as:
49 initial potential= 0.1 V; Final potential=1.0 V; increment potential=0.004 V; amplitude =0.05 V;
50 pulse width=0.2 s; pulse period=0.5 s. Under this optimal condition, effect of concentration of
51 *meta*-cresol on the 6B-PGE* was examined by DPV technique as in Fig. 4A. A systematic
52
53
54
55
56
57
58
59
60

1
2
3 increase in the DPV peak current with increase in *meta*-cresol concentration was observed. To
4 verify the surface adsorption and retainment of the phenol oxidation peak, soon after the *meta*-
5 cresol experiment, the 6B-PGE* is replaced to a blank pH 7 PBS and repeated the DPV (Fig.
6 S2†). If *meta*-cresol is adsorbed on the surface, then, it can be identified as a surface confined
7 peak at 0.55 ± 0.01 V vs. Ag/AgCl in the blank pH 7 PBS. Interestingly, there is no peak signal
8 noticed at 0.55 ± 0.01 V vs. Ag/AgCl with the medium transferred 6B-PGE* (Fig. S2†). This
9 observation specifies absence of any adsorbed product on the surface. Fig. 4B is a calibration
10 plot, showing linearity in a concentration window 40-320 μM with current sensitivity $0.101 \mu\text{A}$
11 μM^{-1} ($1.43 \mu\text{A} \mu\text{M}^{-1} \text{cm}^{-2}$). Beyond 320 μM of *meta*-cresol concentration, saturation in the DPV
12 peak current response was noticed. Fig. 4C, curve a, is a DPV of six repetitive detections of 80
13 μM of *meta*-cresol using 6B-PGE*. A relative standard deviation (RSD) value 0.21% was
14 noticed. Note that, the above repetitive measurements were all carried out without pre-
15 concentration and any interim pretreatment procedures, unlike to the conventional
16 electrochemical sensors.²⁵ Calculated detection limit, D_L (signal-to-noise=3) value is 120 nM.
17 This detection limit and current sensitivity values noticed in this work are better than that of
18 some of the literature reports. For instance, the sensitivity value observed in this work is about
19 2–5 times higher over some of the graphite and biosensors based reports; Kelgraf graphite
20 composite ($0.02 \mu\text{A} \mu\text{M}^{-1}$),¹⁴ GCE/Osmium-poly(1-vinylimidazole)/*tyrosinase* ($0.05 \mu\text{A} \mu\text{M}^{-1}$)¹⁵
21 and Platinum/poly acrylonitrile/polyaniline/*polyphenol oxidase* ($0.06 \mu\text{A} \mu\text{M}^{-1}$)^{32,34} modified
22 electrodes. Likewise, the detection limit calculated in this work is about 300 and 1.5 times lesser
23 than edge plane pyrolytic graphite (30000 nM)⁴¹ and GCE/Osmium-poly(1-
24 vinylimidazole)/*tyrosinase* (156.4 nM)¹⁵ modified electrodes respectively. Although some of the
25 PGE sensors reported in literature have showed slightly better analytical performance in terms of
26
27
28
29
30
31
32
33
34
35
36
37
38
39
40
41
42
43
44
45
46
47
48
49
50
51
52
53
54
55
56
57
58
59
60

1
2
3 higher sensitivity^{42,43} and lower detection limit,⁴³ but in consideration with the followings;
4
5 surface fouling character, simple preparation, reusability and quick operation procedures, present
6
7 system is superior over the aforementioned reports.
8
9

10 11 12 13 **3.5. Interference study**

14
15 Influence of some interfering biochemicals such as ascorbic acid (AA) and uric acid
16
17 (UA) on the detection of 80 μM of *meta*-cresol were next examined as in Fig. 4C, curves a-d.
18
19 Interestingly, without and with addition of 300 μM AA and 450 μM of UA to the above, there
20
21 were no significant alterations in the *meta*-cresol oxidation current signals noticed. The UA gets
22
23 oxidized at 0.3 V vs. Ag/AgCl, and this signal has not influencing the *meta*-cresol detection peak
24
25 existing at 0.55 ± 0.01 V vs. Ag/AgCl. Note that, there is no specific current signal observed for
26
27 the AA oxidation on 6B-PGE* (Fig. 4C, curve b). Presumably, at neutral pH, AA may exist as
28
29 anionic form ($\text{pK}_a = 4.1$) and hence it might be strongly repelled by the anionic oxygen functional
30
31 groups such as $-\text{COO}^-$ and O^- of the 6B-PGE*.⁵³
32
33
34
35
36
37
38

39 **3.6. Real sample analyses**

40
41 Total phenol content in three different commercially available insulin injections, sample
42
43 #1-#3 were tested using 6B-PGE* by a standard addition approach (Fig. 5). Since *meta*-cresol
44
45 and phenol showed quantitatively similar DPV responses at 0.55 ± 0.01 V vs. Ag/AgCl (Fig. 1C),
46
47 for simplicity purpose *meta*-cresol is taken as an internal standard for the measurement of total
48
49 phenolic content in the real samples. Table 2 is the analytical data for quantification of the total
50
51 phenolic content in the real samples, #1-#3. The detected total phenolic content values in the real
52
53 samples are; 2.29, 2.04 and 3.15 mg mL^{-1} . These values were closely matching with the
54
55
56
57
58
59
60

1
2
3
4
5
6
7
8
9
10
11
12
13
14
15
16
17
18
19
20
21
22
23
24
25
26
27
28
29
30
31
32
33
34
35
36
37
38
39
40
41
42
43
44
45
46
47
48
49
50
51
52
53
54
55
56
57
58
59
60

respective labeled values of the real samples, #1-#3. Calculated electrode recovery values are ~100%.

4. Conclusions

An ultra-low cost 6B-pencil graphite preanodized at 2 V vs. Ag/AgCl for 180 s showed efficient differential pulse voltammetric sensing of phenolic preservative/s in the insulin formulations in pH 7 PBS. Oxygen rich functional groups such as phenolic, carboxylic, carbonyl and ether created on the preanodized 6B-pencil graphite surface were found to be responsible for the efficient electrochemical oxidation of the mono-phenols in this work. DPV parameters were systematically optimized. Under an optimal condition, the preanodized 6B-pencil graphite electrode showed linear current response against concentration of phenol in a window 40-320 μM with current sensitivity and regression values of $0.101 \mu\text{A } \mu\text{M}^{-1}$ and 0.999 respectively. Calculated detection limit value was $0.12 \mu\text{M}$. The working electrode can be reusable and renewable without any pretreatment procedures, unlike to the conventional electrodes with series interim surface cleaning steps. Total phenolic content in three different insulin pharmaceutical samples were successfully detected with recovery values ~100%. The developed sensor in this work is suitable for electrochemical detection of various phenols in pharmaceuticals, tea, wine and environmental samples and can be extended as an electrochemical detector in flow injection analysis too.

Acknowledgements

The authors are grateful for the financial support from the Department of Science and Technology (DST) under Technology Systems Development (DST/TSG/ME/2011/16) and DST-

1
2
3 Science and Engineering Research Council (SR/S1/PC-16/2011(G)) for the Raman Spectroscopy
4
5 instrumentation support.
6
7
8
9

10 References

- 11 1 R.M. Barbosa, L.M. Rosario, C.M.A. Brett and A.M.O. Brett, *Analyst*, 1996, **121**, 1789-
12 1793.
- 13 2 C. Guo, C. Chen, Z. Luo and L. Chen, *Anal. Methods*, 2012, **4**, 1377-1382.
- 14 3 Y. Pu, Z. Zhu, D. Han, H. Liu, J. Liu, J. Liao, K. Zhang and W. Tan, *Analyst*, 2011, **136**,
15 4138-4140.
- 16 4 P. Businova, J. Prasek, J. Chomoucka, J. Drbohlavova, J. Pekarek, R. Hrdy and J.
17 Hubalek, *Procedia Engg.*, 2012, **47**, 1235-1238.
- 18 5 G. Danaei, M.M. Finucane, Y. Lu, G.M. Singh, M.J. Cowan, C.J. Paciorek, J.K. Lin, F.
19 Farzadfar, Y.H. Khang, G.A. Stevens, M. Rao, M.K. Ali, L.M. Riley, C.A. Robinson and
20 M. Ezzati, *Lancet*, 2011, **378**, 31-40.
- 21 6 L.S. Rotenstein, N. Ran, J.P. Shivers, M. Yarchoan and K.L. Close, *Clin. Diabetes*, 2012,
22 **30**, 138-150.
- 23 7 W.D. Lougheed, A.M. Albisser, H. M. Martindale, J.C. Chow and J. R. Clement,
24 *Diabetes*, 1983, **32**, 424-432.
- 25 8 C.-H. Hsu, C.-I. Lin and J. Wei, *Circulation*, 2005, **112**, 367-367.
- 26 9 J.L. Whittingham, D.J. Edwards, A.A. Antson, J.M. Clarkson and G.G. Dodson,
27 *Biochemistry*, 1998, **37**, 11516-11523.
- 28 10 S.F. Rajpar, I.S. Foulds, A. Abdullah and M. Maheshwari, *Contact Dermatitis*, 2006, **55**,
29 119-120.

- 1
2
3
4 11 I.V. Faassen, A.M.J.J.V. Vught, M.Z.L. Janousek, P.P.A. Razenberg and E.A.V. Veen,
5
6 *Diabetes Care*, 1990, **13**, 71-74.
7
8 12 V. Clerx, C.V.D. Keybus, A. Kochuyt and A. Goossens, *Contact Dermatitis*, 2003, **48**,
9
10 162-163.
11
12 13 S. Husain, P. Kunzelmann and H. Schildkencht, *J. Chromatogr.*, 1977, **137**, 53-60.
13
14 14 D.E. Weisshaar and D.E. Taliman, *Anal. Chem.*, 1981, **53**, 1809-1813.
15
16 15 O. Adeyoju, E.I. Iwuoha, M.R. Smyth and D. Leech, *Analyst*, 1996, **121**, 1885-1889.
17
18 16 M.T.G. Sanchez, J.L.P. Pavon and B.M. Cordero, *J. Chromatogr. A*, 1997, **766**, 61-69.
19
20 17 K. Nakashima, S. Kinoshita, M. Wada, N. Kuroda and W.R.G. Baeyens, *Analyst*, 1998,
21
22 **123**, 2281-2284.
23
24 18 K. Eggenreich, E. Zach, H. Beck and R. Wintersteiger, *J. Biochem. Biophys. Methods*,
25
26 2004, **61**, 35-46.
27
28 19 S.S. Rane, A. Ajameri, R. Mody and P. Padmaja, *Pharma. Methods*, 2011, **2**, 203-208.
29
30 20 R. Thangaraj, N. Manjula and A.S. Kumar, *Anal. Methods*, 2012, **4**, 2922-2928.
31
32 21 R. Thangaraj and A.S. Kumar, *J. Solid State Electrochem.*, 2013, **17**, 583-590.
33
34 22 S. Menon, N. Vishnu, S.S.S. Panchapakesan, A.S. Kumar, K. Sankaran, P. Unrau and
35
36 M.A. Parameswaran, *J. Electrochem. Soc.*, 2014, **161**, B3061-B3063.
37
38 23 L. Bao, R. Xiong and G. Wei, *Electrochim. Acta*, 2010, **55**, 4030-4038.
39
40 24 J. Mathiyarasu, J. Joseph, K.L.N. Phani and V. Yengaraman, *Ind. J. Chem. Tech.*, 2004,
41
42 **11**, 797-803.
43
44 25 W. Qin, X. Liu, H. Chen and J. Yang, *Anal. Methods*, 2014, **6**, 5734-5740.
45
46 26 J. Wang, R.P. Deo and M. Musameh, *Electroanalysis*, 2003, **23**, 1830-1834
47
48
49
50
51 27 E.J.E. Stuart and M. Pumera, *J. Phys. Chem. C*, 2011, **115**, 5530-5534
52
53
54
55
56
57
58
59
60

- 1
2
3 28 S. Sornambikai and A. S. Kumar, *Electrochim. Acta*, 2012, **62**, 207-217.
4
5 29 V. Carralero, M. L. Mena, A. G. Cortes, P. Y. Seden and J. M. Pingarron, *Biosens.*
6
7 *Bioelectron.*, 2006, **22**, 730-736.
8
9
10 30 L. Wang, Q. Ran, Y. Tian, S. Ye, J. Xu, Y. Xian, R. Peng and L. Jin, *Microchim. Acta*,
11
12 2010, **171**, 217-223.
13
14
15 31 X. Wang, X. Lu, L. Wu and J. Chen, *Chem. Electro. Chem.*, 2014, **1**, 808-816.
16
17 32 H. Xue, Z. Shen and H. Zheng, *J. Appl. Electrochem.*, 2002, **32**, 1265-1268.
18
19 33 D. Shan, C. Mousty, S. Cosnier and S. Mu, *J. Electroanal. Chem.*, 2002, **537**, 103-109.
20
21 34 H. Xue and Z. Shen, *Talanta*, 2002, **57**, 289-295.
22
23 35 H.C.B. Kalachar, Y.A. Naik, S.K. Peethambar, R. Viswanatha and P. Ravindra, *Pharm.*
24
25 *Ana. Qual. Assur.*, 2012, **2012**, 1-4.
26
27
28 36 A.M. Bond, P.J. Mahon, J. Schiewe and V.V. Beckett, *Anal. Chim. Acta*, 1997, **345**, 67-
29
30 74.
31
32
33 37 S. Buratti, M. Scampicchio, G. Giovanelli and S. Mannino, *Talanta*, 2008, **75**, 312-316.
34
35 38 I.G. David, I.A. Badea and G.L. Radu, *Turk. J. Chem.*, 2013, **37**, 91-100
36
37 39 L. Engel and W. Baumann, *Fresenius J. Anal. Chem.*, 1993, **346**, 745-751.
38
39 40 P. Masawat, S. Liawruangrath, Y. Vaneesorn and B. Liawruangrath, *Talanta*, 2002, **58**,
40
41 1221-1234.
42
43
44 41 E.R. Lowe, C.E. Banks and R.G. Compton, *Anal. Bioanal. Chem.*, 2005, **383**, 523-531.
45
46 42 M. Santhiago, C. S. Henry and L. T. Kubota, *Electrochim. Acta*, 2014, **130**, 771-777.
47
48 43 A. Ozcan, *Electroanalysis*, 2014, **26**, 1631-1639.
49
50 44 L. Ozcan, M. Sahin and Y. Sahin, *Sensors*, 2008, **8**, 5792-5805.
51
52 45 A.S. Kumar, S.Sornambikai, S.Venkatesan, J.-L. Chang and J.-M. Zen, *J. Electrochem.*
53
54
55
56
57
58
59
60

- 1
2
3
4
5
6
7
8
9
10
11
12
13
14
15
16
17
18
19
20
21
22
23
24
25
26
27
28
29
30
31
32
33
34
35
36
37
38
39
40
41
42
43
44
45
46
47
48
49
50
51
52
53
54
55
56
57
58
59
60
- Soc.*, 2012, **159**, G137-G145.
- 46 M. Lu and R.G. Compton, *Analyst*, 2014, **139**, 2397-2403.
- 47 J.-M. Zen, H.-H. Chung, G. Ilangovan and A.S. Kumar, *Analyst*, 2000, **125**, 1139-1146.
- 48 A.S. Kumar, S. Sornambikai, P. Gayathri and J.-M. Zen, *J. Electroanal. Chem.*, 2010, **641**, 131-135.
- 49 R.L. McCreery, *Chem. Rev.*, 2008, **108**, 2646-2687.
- 50 N. Vishnu, A.S. Kumar and K.C. Pillai, *Analyst*, 2013, **138**, 6296-6300.
- 51 U.J. Kim, C.A. Furtado, X. Liu, G. Chen and P.C. Eklund, *J. Am. Chem. Soc.*, 2005, **127**, 15437-15445.
- 52 F. L. Encke, *J. Chem. Educ.*, 1970, **47**, 575-576.
- 53 C.X. Lim, H.Y. Hoh, P.K. Ang and K.P. Loh, *Anal. Chem.*, 2010, **82**, 7387-7393.

Figure Captions

- 1
2
3
4
5
6
7 **Fig. 1** Continuous CV responses of 6B-PGE* without (curve a) and with (curve b) 160
8 μM of *meta*-cresol (A) and phenol (B) and its medium transferred responses in a
9 blank pH 7 PBS (curves c in A and B) at a scan rate 50 mV s^{-1} . (C) DPV of 6B-
10 PGE* with 80 μM phenol (b) and *meta*-cresol (a) in pH 7 PBS. Respective
11 chemical structures and plausible electrochemical reactions responsible for the A1
12 and A2 peaks were given as insets. DPV conditions are: initial potential= 0.1 V;
13 Final potential=1.0 V; increment potential=0.004 V; amplitude=0.05 V; pulse
14 width=0.2 s; pulse period=0.5 s.
15
16
17
18 **Fig. 2** (A) Comparative DPV responses of 6B-PGE* (a) and 6B-PGE (b) for the
19 detection of 160 μM of *meta*-cresol and curves (c) and (d) are DPVs of 6B-PGE*
20 with insulin and without *meta*-cresol in pH 7 PBS. (B) CV responses of 6B-PGE
21 and 6B-PGE* with 5 mM $\text{Fe}(\text{CN})_6^{3-}$ in 0.5 M KCl at scan rate 10 mV s^{-1} . (C)
22 Plots of DPV peak current density ($\text{j}/\mu\text{A cm}^{-2}$) values against different grade
23 pencil graphites before (a) and after pre-anodization (b) for the detection of 160
24 μM of *meta*-cresol in pH 7 PBS. Shades of different pencil grades' were
25 displayed as Fig. 2C inset. Other DPV conditions are as in the Fig. 1.
26
27
28
29 **Fig. 3** (A) XRD, (B) Raman and (C) FT-IR spectra of 6B-PGE* (a) and 6B-PGE (b)
30
31 **Fig. 4** (A) DPV responses of 6B-PGE* on successive sensing of 40-400 μM of *meta*-
32 cresol in 10 mL pH 7 PBS, (B) plot of the DPV peak current vs. [*meta*-cresol] and
33 (C) six repeated DPV responses of 6B-PGE* for the detection of 80 μM of *meta*-
34 cresol without (curve a) and with ascorbic acid (AA; curve b), uric acid (UA;
35 curve c) and mixture of UA+AA (curve d) in pH 7 PBS. Other DPV conditions
36 are as in the Fig. 1.
37
38
39 **Fig. 5** Typical DPV responses of 6B-PGE* for the detection of total phenolic content
40 (*meta*-cresol+phenol) in three different pharmaceutical insulin real samples (A-C)
41 by a standard addition approach. Other DPV conditions are as in the Fig. 1.
42
43
44
45
46
47
48
49
50
51
52
53
54
55
56
57
58
59
60

Table 1. Details for the analytical data of various PGE's reported in the literature for monophenols and diphenols detection

Electrode	Activation	Analyte	pH	E_{pa} (V)	Sens. ($\mu\text{A } \mu\text{M}^{-1} \text{cm}^{-2}$)	D_L (μM)	Real Sample	Remarks/limitations	Ref. No
1. H-PGE	Nil	4-nitrophenol	4.0	0.9 ^{#1}	11.3	1.1 ^{#a}	Tap water	<ul style="list-style-type: none"> • Electrode fouling noticed • Single-use type sensor 	42
2. PGE/ Au	Nil	<i>meta</i> -cresol	7.4	0.55 ^{#2}	--	--	--	<ul style="list-style-type: none"> • Electrode fouling noticed • For qualitative detection purpose only. 	35
3. HB-PGE*/ CNT	at 1.4 V for 60 s in pH 4.80	4-octylphenol, 4-nonylphenol & 4-tert-octyl phenol	7.4	0.7 ^{#2}	1.63 0.94 0.53	0.25 ^{#a} 0.42 ^{#a} 0.77 ^{#a}	Effluent	<ul style="list-style-type: none"> • Single-use type sensor • 2 – 12 hrs time required for CNT modification 	38
4. PGE*	at -0.3 to 2.0 V in pH 12.46	Bisphenol	2.0	0.75 ^{#3}	42.2	0.0031 ^{#b}	River water	<ul style="list-style-type: none"> • Pre-concentration procedure involved • Electrode fouling noticed • Single-use type sensor 	43
5. HB-PGE	Nil	Caffeic acid & Trolox	4.0	0.8 ^{#2} 0.5 ^{#2}	--	--	Tea samples	<ul style="list-style-type: none"> • Electrode fouling noticed 	37
6. 6B-PGE*	at 2 V for 180 s in pH 7	<i>meta</i> -cresol & phenol	7.0	0.55 ^{#2}	1.43	0.12 ^{#a}	Pharmaceutical insulin	<ul style="list-style-type: none"> • Fouling free • Renewable/reusable • No pre-concentration 	This work

PGE= Pencil-lead electrode; *= preanodized; CNT=carbon nanotube; DPV=differential pulse voltammetry; #1= vs. Carbon (semi reference); #2= vs. Ag/AgCl; #3=vs. SCE; #a=DPV; #b=Adsorptive Stripping DPV.

Table 2. Analytical result for electrochemical detection of phenolic preservatives in pharmaceutical insulin real samples using 6B-PGE*

Parameters	Sample #1			Sample #2			Sample #3		
	R+S1	R+S2	R+S3	R+S1	R+S2	R+S3	R+S1	R+S2	R+S3
1. Linear equation	$y=0.15+0.102x$			$y=1.75+0.110x$			$y=1.25+0.088x$		
2. Regression	0.981			0.994			0.999		
3. Original detected (μM) (R)	32			19			42		
4. Added (μM) (R+S1-S3)	50	75	100	50	75	100	60	80	100
5. Found (μM)	51	77	99	50.8	73	99.9	59.7	80.6	99.7
6. Recovery (%)	103	103	99.1	101.6	97.3	99.9	99.6	100.6	99.7
7. Detected phenol (mg mL^{-1})	2.29			2.04			3.15		
8. Labeled phenol (mg mL^{-1}) ^{#1}	2.15			2.15			3.00		

R=Real sample; S1-S3= Different standard (*meta*-cresol) concentrations; #1=Total phenol content.

Fig. 1

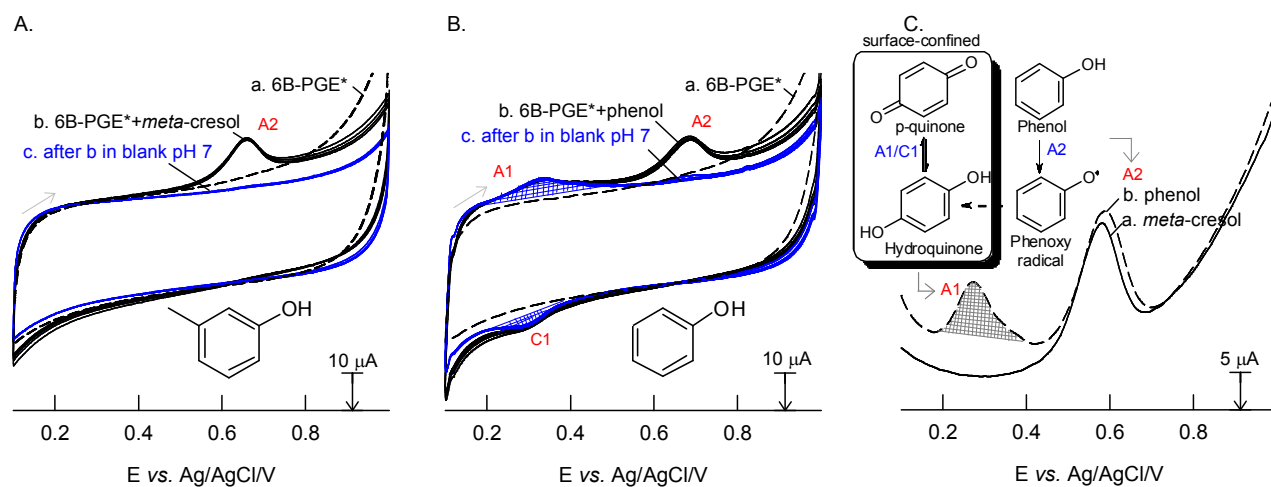


Fig. 1 Continuous CV responses of 6B-PGE* without (curve a) and with (curve b) 160 μM of *meta*-cresol (A) and phenol (B) and its medium transferred responses in a blank pH 7 PBS (curves c in A and B) at a scan rate 50 mV s⁻¹. (C) DPV of 6B-PGE* with 80 μM phenol (b) and *meta*-cresol (a) in pH 7 PBS. Respective chemical structures and plausible electrochemical reactions responsible for the A1 and A2 peaks were given as insets. DPV conditions are: initial potential= 0.1 V; Final potential=1.0 V; increment potential=0.004 V; amplitude=0.05 V; pulse width=0.2 s; pulse period=0.5 s.

Fig. 2

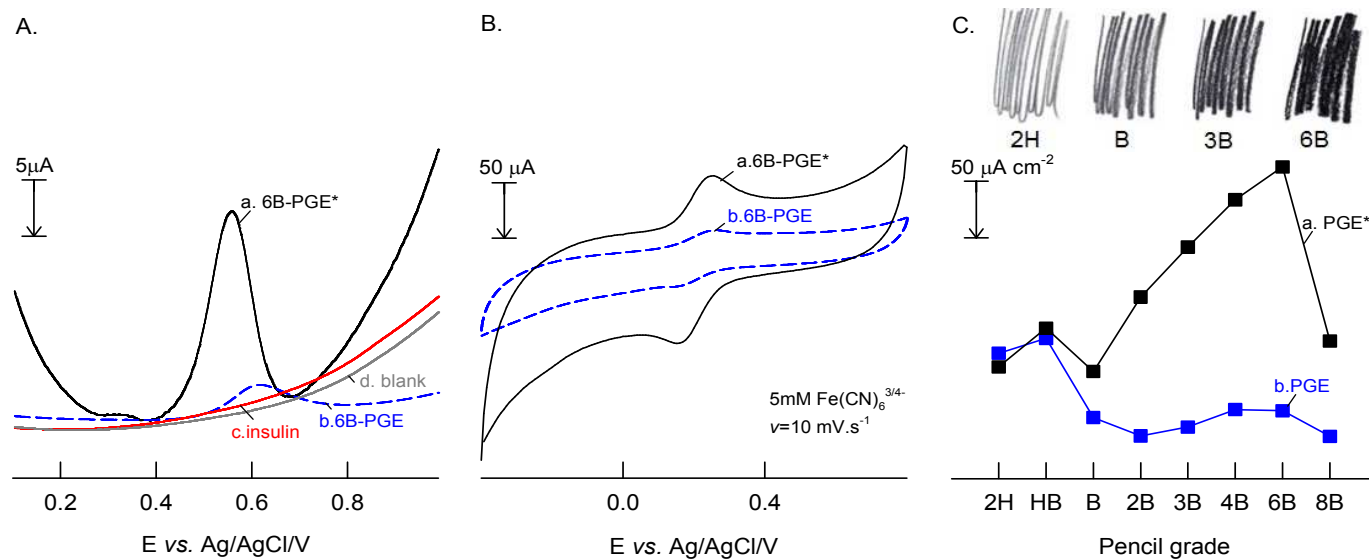


Fig. 2 (A) Comparative DPV responses of 6B-PGE* (a) and 6B-PGE (b) for the detection of 160 μM of meta-cresol and curves (c) and (d) are DPVs of 6B-PGE* with insulin and without meta-cresol in pH 7 PBS. (B) CV responses of 6B-PGE and 6B-PGE* with 5 mM $\text{Fe}(\text{CN})_6^{3/4-}$ in 0.5 M KCl at scan rate 10 mV s^{-1} . (C) Plots of DPV peak current density ($j/\mu\text{A cm}^{-2}$) values against different grade pencil graphites before (a) and after pre-anodization (b) for the detection of 160 μM of meta-cresol in pH 7 PBS. Shades of different pencil grades' were displayed as Fig. 2C inset. Other DPV conditions are as in the Fig. 1.

Fig. 3

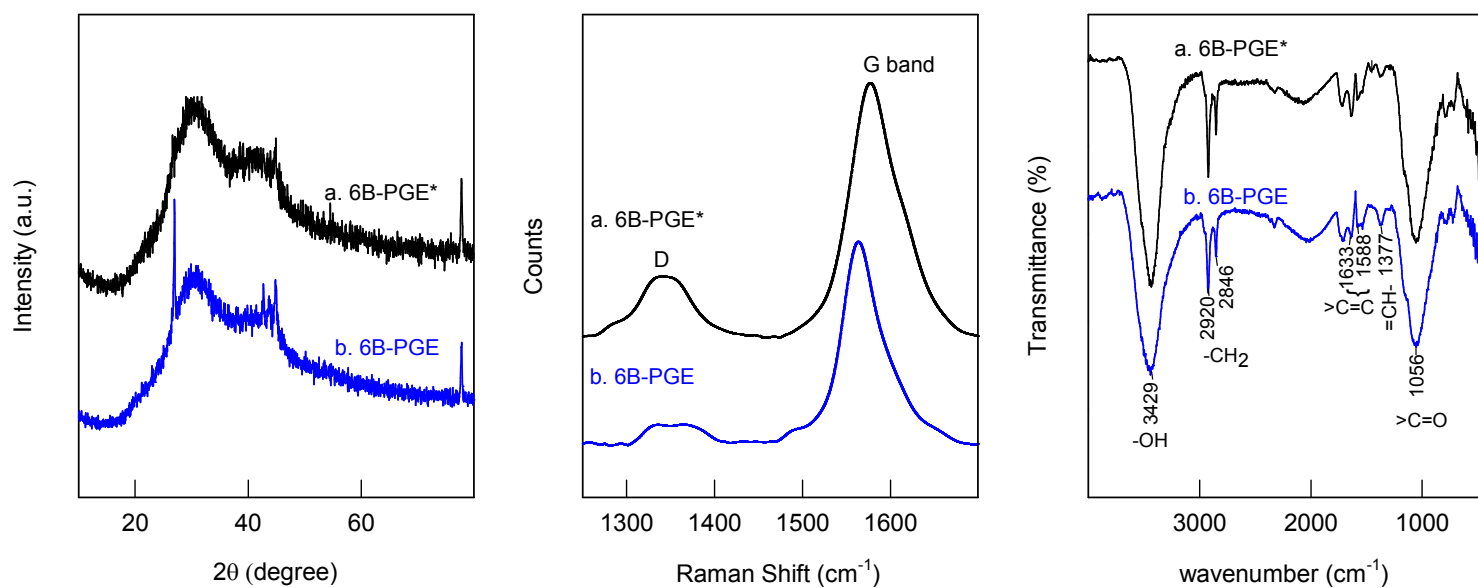


Fig. 3 (A) XRD, (B) Raman and (C) FT-IR spectra of 6B-PGE* (a) and 6B-PGE (b)

Fig. 4

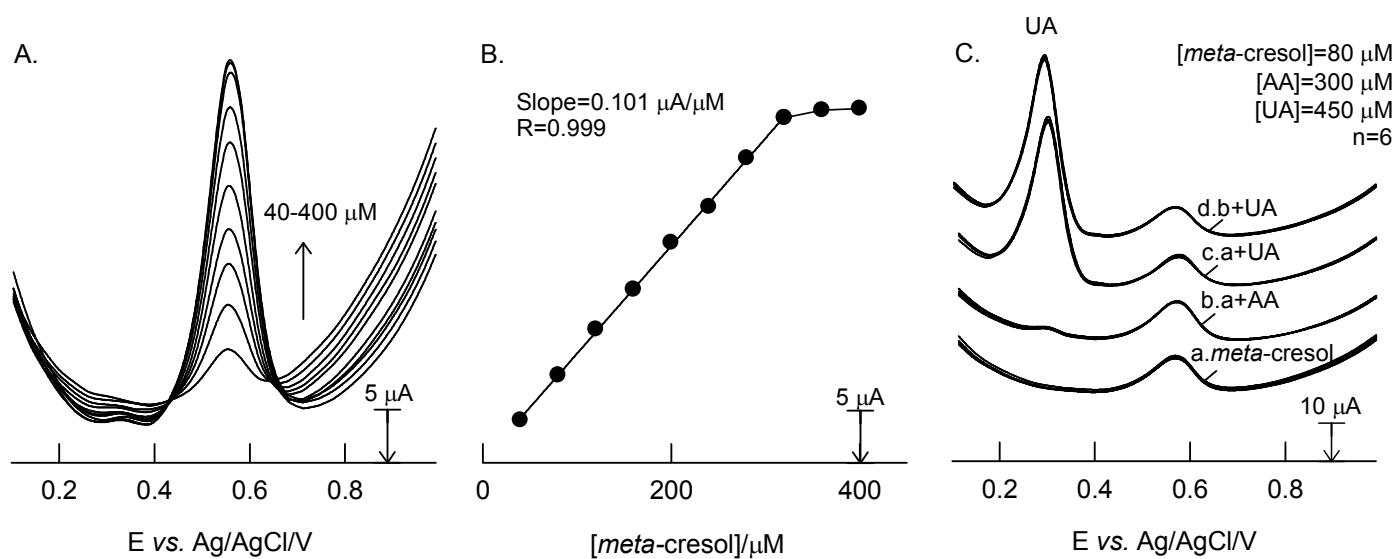


Fig. 4 (A) DPV responses of 6B-PGE* on successive sensing of 40-400 μM of meta-cresol in 10 mL pH 7 PBS, (B) plot of the DPV peak current vs. [meta-cresol] and (C) six repeated DPV responses of 6B-PGE* for the detection of 80 μM of meta-cresol without (curve a) and with ascorbic acid (AA; curve b), uric acid (UA; curve c) and mixture of UA+AA (curve d) in pH 7 PBS. Other DPV conditions are as in the Fig. 1.

Fig. 5

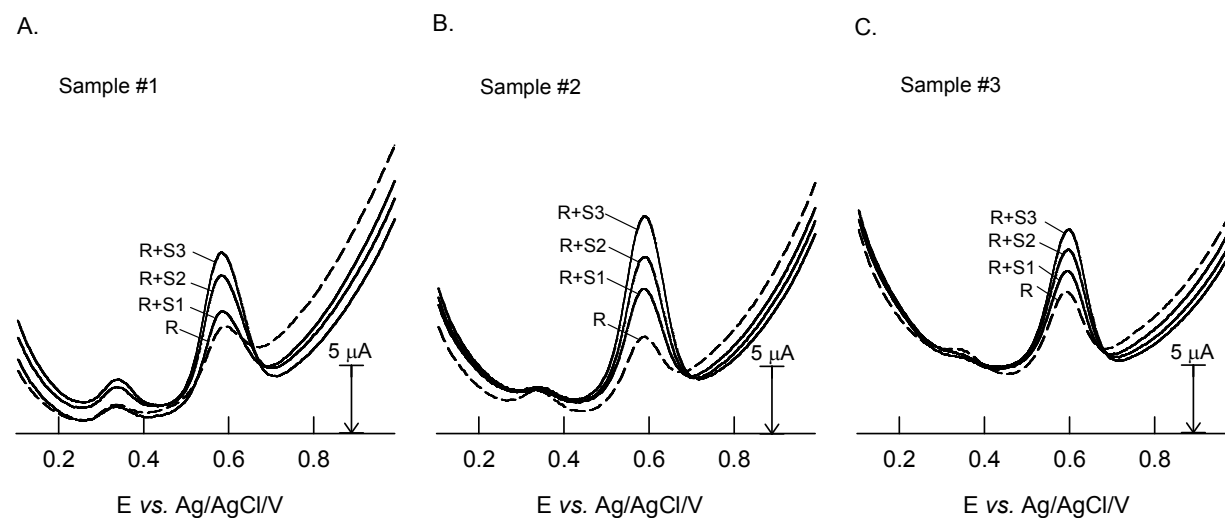
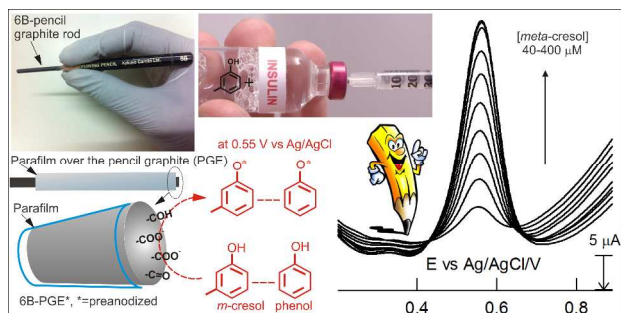


Fig. 5 Typical DPV responses of 6B-PGE* for the detection of total phenolic content (*meta*-cresol+phenol) in three different pharmaceutical insulin real samples (A-C) by a standard addition approach. Other DPV conditions are as in the Fig. 1.

Graphical Abstract (word format)



A low-cost pre-anodized 6B-pencil graphite (6B-PGE*) showed as a fouling-free and renewable electrochemical sensor for mono-phenols and can be used for the detection of mono-phenolic preservatives in pharmaceutical insulin formulations.

